In-situ Growth of Sn-seeded GaAs and GaSb Nanowire Heterostructures

CENTRE FOR ANALYSIS AND SYNTHESIS | LTH | LUND UNIVERSITY | 2023
AZEMINA KRAINA | MASTER'S THESIS IN MATERIALS CHEMISTRY |
MASTER OF SCIENCE IN ENGINEERING, ENGINEERING NANOSCIENCE

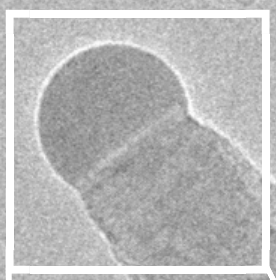

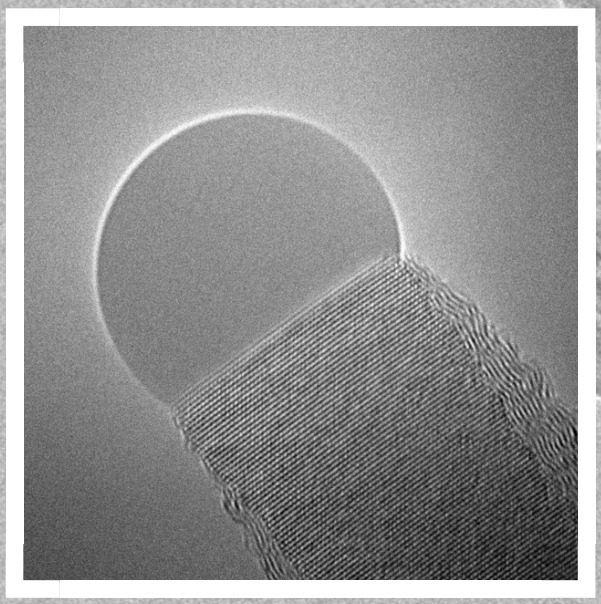

Master's Thesis

Master of Science in Engineering, Engineering Nanoscience

In-situ Growth of Sn-seeded GaAs and GaSb Nanowire Heterostructures

Azemina Kraina

Supervisors:

Miķelis Marnauza, Robin Sjökvist and Kimberly Dick Thelander

Centre for Analysis and Synthesis

Lund University

June 2023

Acknowledgements

There are many people I would like to thank for helping me during my Master's thesis. Firstly I would like to thank professor Kimberly Dick Thelander for giving me the opportunity to join her group, being my supervisor and for always coming with valuable insights.

Moreover, I would like to extend my greatest gratitude towards my co-supervisors Miķelis Marnauza and Robin Sjökvist who have been an immense help during this time. Thank you for the guidance with the experiments, for answering all of my questions, and for teaching me so much about how to think and write like a scientist.

I would also like to thank Daniel Madsen for the help with the ETEM and the rest of the research group for being such nice company and the great discussions at our group meetings.

A special thank you to my examiner Martin Ek Rosén for his interesting questions and comments but also for being the first lecturer to introduce me to crystal structures.

Furthermore a big thank you to Linnéa Jönsson for depositing the Sn-particles on the MEMS-chips.

In a stressful period like this, it is of utmost importance to surround yourself with amazing people, and I have had the pleasure of having the best of friends and boyfriend as my support in Lund. Thank you guys for always being there and enriching my days and my life overall. And thank you Dani for being my light and picking me up at my stressful lows, you mean the world to me.

Last but not least, I would like to thank my dad, mom and brother: Hvala vam od srca za sve, ja nemam reči da opišem koliko mi znači vaša podrška i koliko ste mi pomogli u životu. Bez vas ovo nebi bilo moguče. Volim vas beskrajno.

Abstract

One of the ways to utilize III-V nanowires, is to make use of the possibility to combine materials and create heterostructures which allows for creating material combinations with new properties. A special interest can be taken into Sb-containing nanowires due to the high electron mobility, however there has been reported difficulties with switching to other materials because of a 'memory effect' where Sb lingers in the system and nanowire. Moreover, there is a need for exploring different seed materials such as Sn for nanowires since the commonly used Au can introduce problems in Si-integrated devices. In this thesis, the primary focus was to create heterostructure nanowires of Sn-seeded GaSb and GaAs and try to optimize the transitions by growing nanowires while studying them in an Environmental Transmission Electron Microscope. When growing with GaAs, a twin superlattice structure was detected at a lower V/III ratio versus at a higher V/III ratio where the nanowire grew straight zincblende. This trend seems to coincide with ex-situ work with Sn-seeded GaAs and is exciting since twins can perhaps indicate a possibility for wurtzite to form. Moreover both GaAs-GaSb and GaSb-GaAs were grown and after observing suboptimal switches, such as with substantial overgrowth or kinking, speculations were made as to why these phenomena occurred. These insights helped with the succeeding growth of GaSb-GaAs-GaAsSb heterostructures. For the GaSb-GaAs switch, the ability to switch to pure GaAs was an intriguing discovery as there has not been any record of this before. However the transitions in the GaSb-GaAs-GaAsSb heterostructure observed were gradual, and for the first switch (GaSb-GaAs) the nanowire kinked and in the second switch (GaAs-GaAsSb) As never fully left the nanowire crystal. This work has contributed to the understanding of the different roles the parameters play in terms of affecting the GaAs and GaSb heterostructure nanowire growth, but also laid a foundation for future research.

Contents

List of Abbreviations

MOCVD - Metal-Organic Chemical Vapor Deposition
TEM - Transmission Electron Microscope
ETEM - Environmental Transmission Electron Microscope
NW - Nanowire
ZB - Zincblende
WZ - Wurtzite
HCP - Hexagonal Close Packed
FCC - Face Centered Cubic
TMGa - Trimethylgallium
TMSb - Trimethylantimony
VSS - Vapor-Solid-Solid
VLS - Vapor-Liquid-Solid
STEM - Scanning Transmission Electron Microscope
FFT - Fast Fourier Transform
EDX - X-ray Energy Dispersive Spectroscopy
MEMS - Micro Electro Mechanical Systems

1. Introduction

At the nanoscale it is possible to use unique properties such as high surface to volume ratio and the possibility to combine materials which in bulk form are incompatible. A popular way of making use of these properties are nanowires; rod-like structures with diameters in the nanometer scale while the length can be in the micrometer scale. One approach of creating nanowires is by Vapor-Liquid-Solid method (VLS) where the material is supplied in gas form, and there are liquid seed particles being the starting point for nucleation of solid nanowires. III-V nanowires, consisting of group III and group V elements, are widely researched and could be used for electronic devices and photonic applications [1]. An example of especially interesting III-V materials are III-Sb nanowires that have high carrier mobilities and a narrow bandgap which makes them suitable for applications such as quantum transport, thermoelectronics and low-power electronics. However, III-Sb nanowires are not as well researched as other group III-V nanowires, such as III-As and III-P. This is mainly due to the low vapor pressure of Sb meaning it lingers in the system and its surfactant effect - meaning there is an influence on the surface energies of the materials present, which will intervene with e.g. nanowire nucleation, growth dynamics and crystal phase selection [2].

An interesting way of using Sb is by combining different materials with each other creating heterostructures [1]. There is a considerable amount of research on nanowire heterostructures, and common difficulties are e.g. lattice mismatch between the materials leading to strain and defects [3]. Research by M. Borg et al. [4] with ex-situ Metal-organic Chemical Vapor Deposition (MOCVD) studies of growing Au-seeded GaAs-GaSb, showed that when switching to GaSb there is a radial increase since there is an increased uptake into Au particle. Moreover, when growing heterostructures with Sb, and switching to a material without Sb, the growth can be suboptimal depending on the aim for the growth. This is due to the aforementioned surfactant effect, and results in a graded interface where Sb is present in additional layers even if no further Sb is supplied. Since the Sb lingers it is termed as a 'memory effect' [2].

When performing nanowire synthesis, there are many aspects to consider. For example when using particle-assisted VLS growth, there needs to be an assessment of the most suitable seed material, in addition, it is also important to decide what instrument setup to use for the growth. A common seed material is Au, however it is costly and it is not optimal for devices based on Si due to the ability to introduce unwanted electronic states in the band gap. Another option which is compatible with Si-based semiconductor processing, is Sn. Sn has also been shown to be more compatible with Sb-containing material [5].

There are examples of ex-situ studies of growing Sn-seeded GaAs [6] and Sn-seeded GaAs-GaSb junctions [5] by MOCVD. There is a lack of research that has focused on examining switch from pure III-Sb to III-As, most likely due to the difficulties of the

memory effect mentioned above, however, considering that GaSb has such a high hole mobility, there is a possibility to create for example quantum dots in combination with other materials which makes it of interest to examine.

2. Goal

The limitation of growing nanowires to then study them afterwards is that there is no way of knowing how e.g. the nanowire growth process takes place. However the growth can also be studied as it is occurring, 'in-situ', with instruments as for instance an Environmental Transmission Electron Microscope (ETEM), which can take form as a TEM connected to a MOCVD system. This means that different reactions and processes such as oxidation, reduction, nucleation and crystal growth can be studied in real time. Therefore changes can be directly implemented and evaluated to the parameters that can be controlled such as temperature and gas flows[7]. In spite of the lack of published research of GaSb to GaAs transitions, a promising way of studying the growth is in-situ with an ETEM since the purpose would be to try to optimize and find ideal growth conditions.

In this project the goal was to study and try to optimise growth parameters 'in-situ' for successful transitions of heterostructures, Sn-seeded III-V materials GaAs and GaSb. Both GaAs-GaSb and GaSb-GaAs were to be explored and studied with a special focus on GaSb-GaAs since there is a lack of understanding and reports of successful transitions.

3. Background

The following theory and instruments will be described in order to provide context for understanding the findings in this thesis: Metal Organic Chemical Vapor Deposition (MOCVD), the theory of nucleation and growth of nanowires and their crystal structure in order to make it clear what nanowires are and how they can be grown. Following that, the techniques used to study nanowires such as Transmission Electron Microscopy and Scanning Transmission Electron Microscopy together with Energy Dispersive X-ray spectroscopy will be introduced. Finally the combination of growth system and microscope will be described - Environmental Transmission Electron microscopy.

3.1. Metal-organic Chemical Vapor Deposition

Metal-organic Chemical Vapor Deposition (MOCVD), is used for growth of materials such as semiconductor crystals. A setup with metal-organics, such as Trimethylgallium

(TMGa), Trimethylantimony (TMSb) and hydride precursors, such as arsene (AsH_3), containing the wanted elements can be used where the metal-organic precursors are stored in so called bubblers and can appear in either solid or liquid form. When hydrogen flows through the metal-organics, the gas becomes saturated with the precursor and can be led to the chamber while the hydrides can be directly led to the chamber. A schematic of an MOCVD setup is shown in Figure 1 [8].

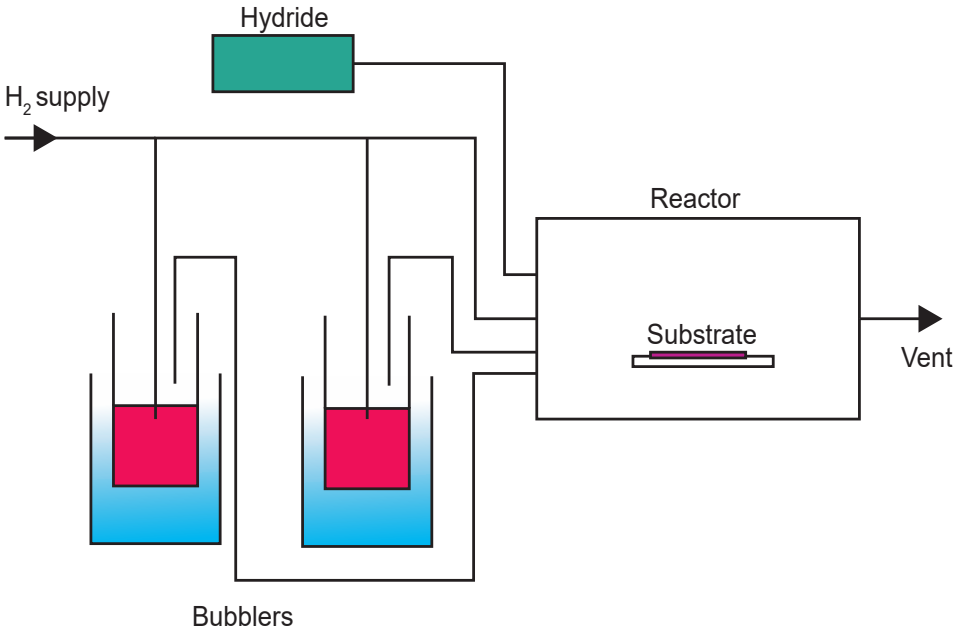

Figure 1: Schematic of a MOCVD setup.

In the chamber there is a heated substrate where the the elements wanted for the growth are released when the gaseous, unstable, precursors come close and dissociate, often mentioned as pyrolytic mechanisms. There are multiple factors that influence this mechanism, such as temperature, what precursors are present, pressure and surface structure. This can be used to tune and optimize the growth of the materials for different applications [8].

3.2. The principle of particle assisted nanowire growth

MOCVD is one of the common ways to grow nanowires. Growing particle assisted nanowires differs from growing bulk epitaxial crystalline layers, however there are several similarities and the general procedure will firstly be described in order to give a foundation for understanding nanowire growth.

3.2.1. Thermodynamics and kinetics

Driving forces of reactions and phase transitions are governed by thermodynamics, where chemical potential differences can help promote for example crystal growth, although there can also be kinetic barriers which will be discussed later. The partial derivative of Gibbs free energy defines, μ_k, which is the chemical potential for a distinct component with a specific amount n_k, at a set pressure, P and temperature T and with a unchanging amount of possible other components in a general system, $n_{j\neq k}$ [8].

$$\mu_k = \left(\frac{\partial G}{\partial n_k}\right)_{T,P,n_{j\neq k}} \tag{1}$$

For various phases of the same material, it is not certain that they have the same chemical potential which will drive the system to produce the more energetically favorable phase. In a system with only one type of material in vapor and solid phase, then the variation in chemical potential between the two can be expressed as in Equation 2, where μ_v is the chemical potential for the vapor phase and μ_s if for the solid phase. The P is the partial pressure and P_0 is the equilibrium partial pressure. This equation shows the important concept of supersaturation ($\Delta\mu$) and the higher the supersaturation, the more the system is pushed from equilibrium and the more favored the solid will be, i.e. crystals will form [8].

$$\Delta\mu = \mu_v - \mu_s = RTln(P/P_0) \tag{2}$$

In theory it is possible to calculate and attempt to predict the outcome of different systems based on thermodynamic equations, however, this is only for ideal cases where no other factors can affect the system. In addition to thermodynamics, kinetics also play an extensive role in governing the reactions and transformations that take place in a system. Some examples of this is the mass transport which entails the flow of the material. This combination of effects make it difficult to predict the outcome of different reactions and systems, since there are even more aspects to consider and growing nanowires is even more complicated [8].

3.2.2. General nucleation

In for example a MOCVD setup, crystal growth occurs from the vapor to solid phase, i.e. crystal growth that takes place is a phase transformation to a solid organized structure. In the beginning of the phase transformation, the smallest part considered a crystal is a metastable nucleus, and the Gibbs free energy shown in Equation 3 (ΔG_N), needs to be negative for solidification to occur. ΔG_V is the energy for the volume of the nucleus, ΔG_S is the energy for the area of the phase boundary created and ΔG_E is the energy term for

if the nucleus is exposed to elastic stress [8].

$$\Delta G_N = \Delta G_V + \Delta G_S + \Delta G_E \tag{3}$$

The volume term in Equation 3 is negative since creating a new volume of the preferred phase when the system is supersaturated is thermodynamically favorable, however, the surface term is positive since it costs energy to create new surfaces. Moreover the elastic stress term is positive if the system is subjected to elastic stress by e.g. having a substrate of a different material than the nucleus. It is important to note that there is a critical radius for a nucleus to form, meaning that if it is any smaller than said critical radius it will not form which is also illustrated in Figure 2 as **r*** [8].

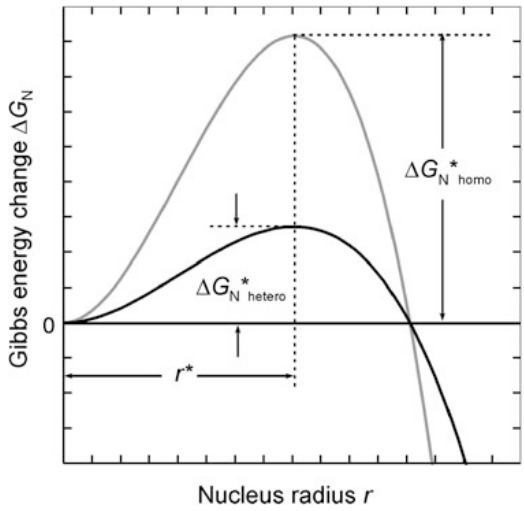

Figure 2: Gibbs free energy diagram showing the critical radius, taken from [8].

In homonucleation the solid nucleus forms in a homogeneous phase of the same material, while in heteronucleation there are some preferable sites for nucleation.

3.2.3. Nucleation and growth of nanowires

After the introduction of the general thermodynamics and nucleation process, the principle of particle assisted nanowire growth can be described. A prevalent method implemented to grow nanowires is to use a seed particle, either in solid or liquid form. If a solid particle is used it is called the Vapor-Solid-Solid (VSS) method, and using a liquid particle is the Vapor-Liquid Solid (VLS) method. In this thesis the focus will be on seed particles in the liquid phase. Other than the liquid term L in VLS, the vapor (V) part stems from the fact that gasses are added in the vapor phase and the solid (S) part from the crystalline parts that form in the solid phase. The mechanism was first proposed by Ellis and Wagner in 1964, after observing Si whiskers grown using Au seeds [9]. By

using an experimental method such as MOCVD described in Section 3.1, and having a heated substrate with seed particles, when the precursors enter the reaction chamber, the wanted materials are released via dissociation. They can then alloy with the particle that can act as a reservoir. At the point of supersaturation there is a thermodynamic driving force for solidification, and nucleation of a crystalline material made up of the precursors can occur. The seed particle has been seen to act as a preferential site for nucleation of the precursor materials and forming a crystal at the substrate-particle interface at first and then the growth continues in the particle-nucleus interface, see Figure 3. There have been suggestions that the nucleation starts at the three-phase interface, meaning the edge of the particle-substrate interface. In order for the growth to be thermodynamically favorable, the vapor has to be supersaturated compared to the particle and the particle supersaturated compared to the substrate [10].

In MOCVD there is a constant source of precursor gasses that flow onto the substrate in the reaction chamber. This results in a condition that is in a steady state and growth of e.g. new layers in nanowires, can continuously occur [10].

Other than the thermodynamic forces described above, there are kinetic factors determining the rate of the process as well. An example of a factor is that there are several ways for the material to reach the nanowire, and many places where precursors can crack, which are illustrated in Figure 3. This can also show the different paths the precursors can take, i.e. adding to the nanowire but also incorporating in islands or surface growth instead. Precursor atoms can enter the particle to be absorbed or atoms can desorb from the particle (1) or to/from the wire directly (4), atoms can diffuse on the side of the nanowires into the particle and be joined into the wire (2), or diffuse by the nanowire (3) adding to islands/surface layers (5) [11]. In Figure 3, it is also shown a zoomed in schematic of how it can look like when new crystal layers form in a nanowire as it is growing.

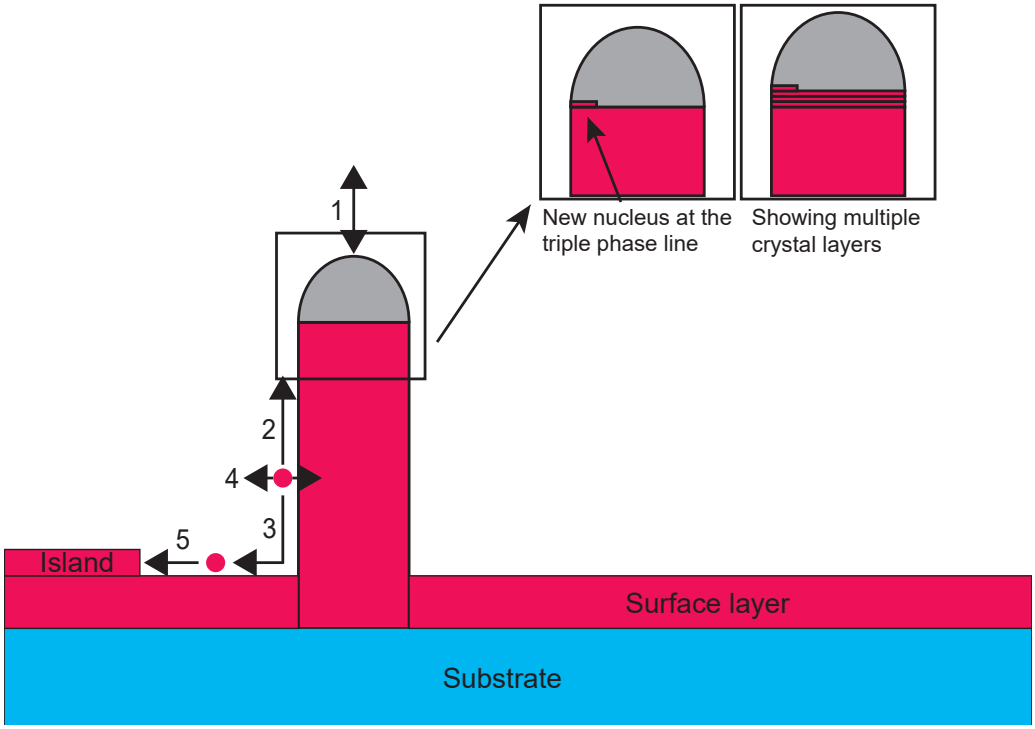

Figure 3: Schematic of nanowire growth.

3.3. Crystal structure in nanowires

III-V materials can in bulk generally form zincblende (ZB), however, when grown as nanowires they can also grow in the wurtzite (WZ) crystal structure. The ZB structure has a cubic unit cell and in stacking it can be seen with an ABCABC layer pattern, while the WZ structure has a hexagonal unit cell and in stacking ABAB structure. [12]. The layers are shown in a schematic in Figure 4, [111]/[0001] direction which would coincide with the preferred growth direction of nanowires.

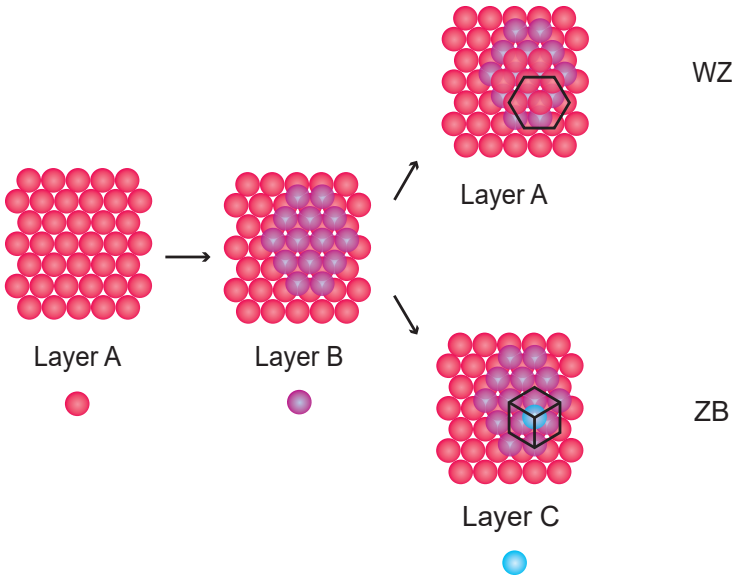

Figure 4: Showing the layer structure for WZ (hcp) and ZB (fcc).

When studying nanowires, there are certain directions that can illustrate these differences in stacking layers very clearly and some of these are shown in Figure 5. Note that the ABCABC vs ABABA pattern is shown in the figure and that every layer is a bilayer of e.g. a group III and V material, and can also be written like AaBbCc, where the small letter is the group V atom.

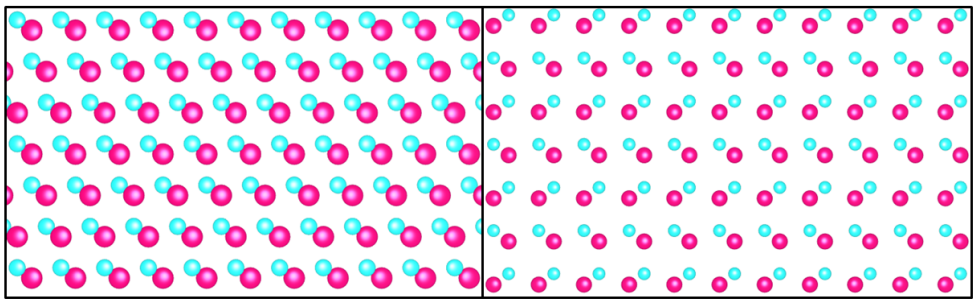

Figure 5: The left panel illustrates the atomic stacking pattern of ZB crystal structure, with the viewing direction as [1-10] and the [111] growth direction going up in the figure. The right panel depicts the atomic stacking arrangement within the WZ crystal structure, showcasing the viewing direction as [11-20] with the [0001] growth direction going up in the figure.

The wurtzite structure is metastable and is not seen for most materials in bulk form which makes it of interest to explore and research. Since it results in a changed band structure of the material compared to zincblende, it is of great interest to use these properties for electronic and optical applications [10].

3.4. Transmission Electron Microscopy

A Transmission Electron Microscope (TEM), where a parallel beam of electrons passes through a sample, is optimal for studying nanowires due to the possibility for angstrom resolution. The crystal structure of nanowires can be identified via imaging but also by using diffraction. In this section the basic principles of a TEM are described, how electrons interact with the sample and the main components of a general TEM.

3.4.1. Beam Interaction with sample

There are several types of interactions that the electrons undergo when they interact with the sample. One way of categorizing them is elastically versus inelastically scattered electrons. Elastically scattered electrons have not transferred kinetic energy to the sample atoms without losses when interacting with the sample, while the opposite is true for inelastically scattered electrons. The beam electrons can also be divided into coherent and incoherent after passing through the sample, referring to whether there is a defined phase relationship with the incident beam or not [13].

3.4.2. Main components of a TEM

A common electron gun to use is a cold field emission gun (FEG) which works by having a very small tip, in the range of µm, which acts as a cathode of for example tungsten. By applying an electric field, electrons can be extracted from the tip. If the applied electric field to the tip is strong enough - the potential barrier for the electrons to escape decreases and electrons can tunnel out of the tip. This phenomenon is termed as field emission and it can occur at room temperature or at heightened temperature. If the former is true it is called a 'cold' FEG. Subsequently when the electrons have been emitted from the tip, they can be accelerated up to 80-300 keV in order to reach and transmit through the sample. This is done by using an anode that will force the electrons to accelerate due to the potential difference [13].

In the TEM column, after the electron gun, there are multiple lenses and apertures which can be seen in Figure 6. Firstly, there is a condenser lens system which forms the initial beam spot and allows for changing the size of the electron beam that interacts with the sample. Then there is a condenser aperture that allows control of the amount of high angle electrons and general number of electrons that will interact with the sample. After this comes the specimen stage where the sample is mounted, and underneath an objective lens which forms the initial image of the sample and an objective aperture which is located in the back focal plane of objective aperture allowing us to select a specific spot(s) in the diffraction pattern. Following this there is a selected area aperture which is located in the image plane of the objective lens allowing to select an area to

acquire a selected area electron diffraction pattern. And lastly there is an intermediate lens system which allows to select the real space or reciprocal space image contained in the image or back focal plane of the objective lens and magnify the image along with a projector lens system which projects the image on a screen/camera [14].

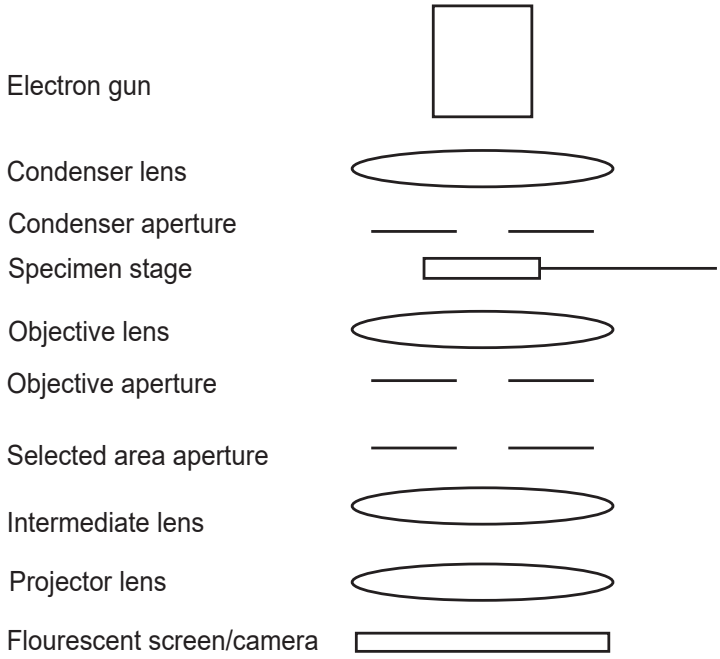

Figure 6: Schematic of a general TEM.

When observing a TEM image the contrast that appears can be split into two categories, amplitude and phase contrast. Amplitude contrast both entails mass-thickness contrast and diffraction contrast. Mass-thickness contrast arises due to the atomic number, or the thickness of the sample which will both affect the scattering of electrons - in an image, thicker regions or regions containing higher Z atoms, will be darker than thinner regions. Secondly there is diffraction contrast, and this type of contrast only arises in crystalline samples due to the crystal lattice, where the electrons can be diffracted according to Braggs law. This creates a diffraction pattern in the back focal plane. Lastly there is phase contrast, this stems from the electrons behaving like a wave, interacting with the atoms within the specimen. Phase contrast images are created when multiple waves are allowed to interfere, as they travel different paths they create an interference pattern on the image plane. This is the contrast that allows to obtain atomic resolution images, which is optimal for studying the crystal structure of for example nanowires. Phase contrast is also extremely useful when trying to do alignment of a TEM, as it creates Fresnel fringes which can be seen as white edges (underfocus) or black edges (overfocus) and this is an indication of how to focus correctly [13].

3.4.3. Scanning Transmission Electron Microscopy

An alternative to a conventional TEM is a Scanning Transmission Electron Microscope (STEM), which works by having a focused beam that is raster scanned and then an image is constructed point by point. This allows STEM mapping with different regions of a sample. Moreover it allows for studying mass-thickness contrast at atomic resolution [15].

A conventional TEM can be converted into STEM by having an additional objective lens above the sample that can focus the beam, having scanning coils that can guide a probe over the sample, and detectors for recording signals that can be turned into images. The detectors are generally a bright field (BF) detector for electrons that have not been scattered at high angles as well as an annular dark field (ADF) detector, that detects electrons that have scattered at high angles. The ADF detector is used to create images with pure mass thickness contrast which can give atomic resolution, compared to high resolution TEM (HRTEM) which is based on phase contrast [15].

3.5. Energy Dispersive X-ray spectroscopy

Energy Dispersive X-ray spectroscopy (EDX) can be used in order to obtain the elemental information about a sample. When the beam of electrons hit the sample (see 1 in Figure 7 below), there is a possibility for them to reach the core electrons of an atom. If the beam electron transfers enough energy to eject a host atom electron (2 in Figure 7), the atom will be excited leading to a higher shell electron relaxing to the lower shell (3 in Figure 7). When this occurs, the energy lost from the electron changing states is either emitted as an Auger electron or an X-ray (4 in Figure 7). In both cases the energy is characteristic of the elements the sample contains. In EDX, the X-rays are of interest, and by using a detector to collect and analyze them the composition can be examined. There are also non-characteristic X-rays; when electrons pass close to the nucleus they can loose a significant amount of energy, which also generates X-rays and will create a background in an EDX spectrum. These types of X-rays form a continuous spectrum and are termed *Bremstrahlung* [13].

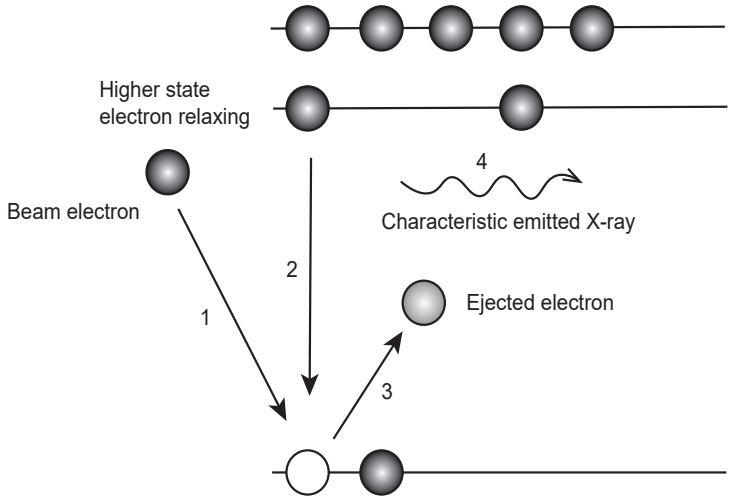

Figure 7: Schematic of how a beam electron can eject a host electron, causing a higher energy electron to relax, resulting in an emitted X-ray.

In order to collect the X-rays a detector is needed, and the most common one used today, and also the one used in the experiments of this thesis, was a Si drift detector (SDD). It is made of high purity silicon and takes the shape of p-doped rings arranged in an array around an n-doped anode. The principle is that when an X-ray hits the detector that has a bias applied, the X-rays can be translated to an electron cloud when electron-hole pairs are created, and the charge of the cloud corresponds to the X-ray energy. The electrons then drift to the anode where the charge can be converted into a voltage signal which in turn is converted into counts [13].

There are different transitions available between the shells, some are more probable than others and will therefore have different relative intensities. Transitions to specific shells have special appearances, and are called families. The most intense peaks are the K-family, then the L-family and lastly the M-family, but not all may be visible in the energy range depending on the element. These peak values can then be compared to tabulated ones to identify the elements present. It is important to recognize certain peaks which could be a misleading representation of the specimen, so called artifact peaks. These peaks can come from the detector, for instance if two X-rays enter simultaneously then the energy detected would be the sum of them. Moreover since the detector consists of Si, there can be internal fluorescence peaks, but also X-rays that enter the detector from the specimen can excite Si meaning the energy detected would be lower by the Si K peak [13].

EDX can also be used as a tool to calibrate temperatures of samples, this is important

since sample properties such as thickness and morphology can vary. The first peak, closest to zero in energy, is called the strobe peak and originates from the detector being able to pick up photons from black body radiation from the chip, meaning it is correlated to the temperature [7].

When the elements present have been identified, quantification is possible, and the procedure is the following. The intensity of the peaks visible in an EDX spectrum depends on the concentration, and by subtracting the background, comparing peaks relative to each other and integrating the counts it is possible to use the Cliff-Lorimer ratio, see equation 4. C_A and C_B are the concentrations of the elements present, k_{AB} is the sensitivity factor, I_A and I_B are the integrated intensities of the elements. The sensitivity factor is not a constant and depends on the setup used and it is material specific [13].

$$\frac{C_A}{C_B} = k_{AB}\frac{I_A}{I_B} \tag{4}$$

3.6. Environmental TEM

With a TEM it is possible to get atomic resolution micrographs, however when studying the sample it is under vacuum and there is no possibility to view processes in real time. By using an Environmental Transmission Electron Microscope (ETEM), it expands the analysis possibilities even further. In the ETEM used in this thesis the TEM is connected to a specialized MOCVD system, see Figure 8, which is optimized for nanowire growth and it is an open cell environment meaning that gas is supplied directly into the microscope chamber. The ETEM allows for control of temperature and gas flows while simultaneously studying samples with atomic resolution. Moreover there is a STEM unit installed which enables another way of analyzing the sample, including a BF and ADF detectors. There is also a secondary electron (SE) detector that enables visualizing the topography and complements the ADF images. Together with the EDX detector there can be STEM mapping of the specimen, however the lens that is forming the probe is not aberration corrected [16].

The MOCVD system connected to the TEM can provide different materials to the specimen (TMGa, TMSb, AsH_3 etc.) and this allows for up to 6 Pa near the sample. There are different pumps in place to remove the excess gas, since this can drastically damage the electron gun by depositing material onto it [16].

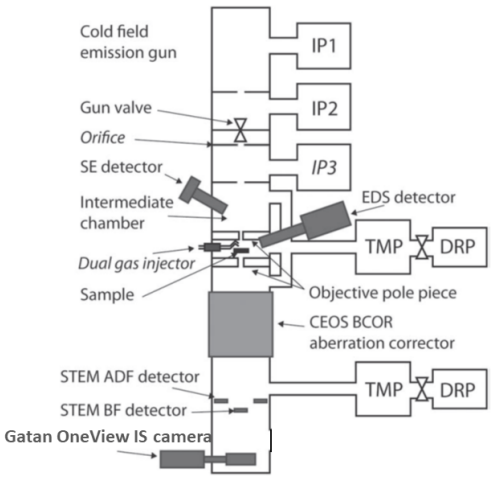

Figure 8: Modified ETEM schematic from C. Hetherington 2020 [16].

4. Experimental Methods

The samples used were Micro Electro Mechanical Systems, MEMS, chips with deposited Sn particles. These samples were then loaded in a Hitachi HF-3300S ETEM, a TEM with a connected MOCVD system enabling observation of crystal growth. By using high resolution TEM and doing STEM-mapping to obtain images and videos of the system, and EDX to obtain the composition, information about the growth dynamics and both seed particle and nanowire composition was collected. Below is a more in depth description of the MEMS chips and particles as well as information about the EDX procedure. Moreover the procedure for switching between different materials is explained.

4.1. Chips and particle deposition

The MEMS chips have 19 holes as shown in Figure 9, where there is a thicker SiN_x region, a thinner SiN_x region in the holes and vacuum in the middle [17]. It is ideal to image atomic resolution structures in vacuum as there is no interference from an amorphous film behind.

The tin particle deposition on the MEMS chips was done by fellow researcher Linnea Jönsson using spark ablation. The spark ablation process includes using two electrodes of a metal or semiconductor material and applying a high voltage, which generates a spark making the electrode material evaporate. This evaporated material can then

nucleate and agglomerate and be compacted in a furnace, size selected and then deposited on the wanted substrate [18]. Several different MEMS chips were used with varying particle density: 2, 4, 8 μm^{-2} but the same diameter of 30 nm.

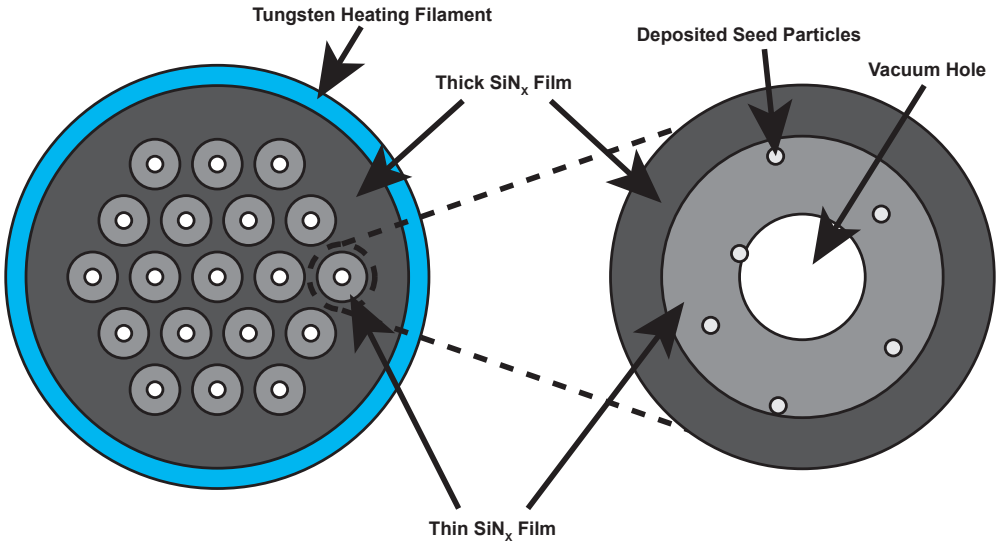

Figure 9: Modified schematic made by Aidas Urbonavicius of a Norcada MEMS chip.

4.2. Using EDX in the experiments

To receive information about the composition of wire and particle as the nanowires were growing, TEM-EDX was used, i.e. the area probed was as big as the beam illuminating the specimen. The resulting spectrum is for a specific area [13].

During some experiments STEM-EDX was used to study the overall composition. A STEM-EDX spectrum can be collected of a single point, a line or a map. In contrast to gathering an EDX spectrum from an area with TEM where the information is not spatially resolved, STEM mapping with EDX is a powerful tool and can give an entire overview of a structure. This allowed for visualizing and receiving information about for example transitions of different materials. When acquiring map spectra it is important to acquire signal for as long as possible, to receive many counts and therefore a more reliable result [15].

4.3. Growth process and preparing for a switch

The general growth occurs by heating up the chip to several hundred degrees, and flowing in gasses at predetermined flows. The goal was to nucleate the Sn particles and start growing axial nanowires, and if this was not occurring the temperature and/or gas flows were changed, one parameter at a time. In order to see if the nanowires were growing in steady state conditions, the nanowires were examined qualitatively to see if the growth was stable and there were no changes, when there were no changes of the growth parameters.

When creating heterostructures, there is a need for switching gas materials in the gas system in a suitable way and there is a common procedure to follow. Firstly, the temperature was lowered to 150 °C in order to prevent further cracking of precursors within the chamber. Subsequently, the gas supply to the chamber was stopped. There are two inlets, one for group III precursors and one for group V, meaning that the same lines were used for AsH_3 and TMSb. Due to the residual gas in the lines, they were most times purged, meaning that they were flushed with nitrogen gas. The ETEM system includes a Residual Gas Analyzer, a mass spectrometer that somewhat represents the composition in the chamber as it is located at the exhaust. The values of the different precursors were studied and as they were lowered and/or stabilized, this helped decide when to start supplying new material.

5. Results and Discussion

In this section there is a description of the results found in the experiments, focusing on growth of Sn-seeded GaAs and GaSb along with forming heterostructures of the aforementioned materials. Findings, difficulties and the process will be discussed along with possible reasons for observed outcomes and comparisons with pre-existing research.

5.1. Growth of GaAs

There were several attempts at nucleating GaAs, and nucleation was possible at a wide range of temperatures ranging 260 to 415 °C. The temperature was both ramped up in order to find a temperature where it nucleates but also ramped down to find an upper limit, during different experiments. This seems promising for Sn-seeded GaAs wires, since there is a wide range of temperatures that can be explored. There were not many issues with starting to nucleate however there were some difficulties during the actual nanowire growth which will be discussed later, but nonetheless there were some interesting discoveries in the nanowires that were observed. In one of the experiments, using a temperature of 385 degrees, and working with different V/III ratios a nanowire

and its morphology was studied. With a V/III ratio of 560 the wire grew vertically, straight with no kinks, see panel (a) in Figure 10. When decreasing the V/III ratio to 280, there were twin planes formed and as seen in panel (b) and (c) in Figure 10 there is a twin superlattice structure. The results are also shown in Table 1.

Table 1: V/III ratio and resulting nanowire appearance at 385 °C.

V/III ratio	560	280
Resulted in	Straight	Twinned

This trend seems to coincide with the work of Rong. S et al. [19], where Sn-seeded nanowires were grown ex-situ on GaAs(111)B-substrate and a lower V/III ratio resulted in twinned nanowires while a higher V/III ratio resulted in straight nanowires. The nucleation event of the crystalline layers determines the crystal structure, for example governing whether it is WZ or ZB [20]. There are several factors affecting which crystal structure that forms, e.g. surface energies and supersaturation [21]. An interesting aspect of the twin planes is that it indicates a possibility for polytypism since there have been some observations of twin planes in the transition from zincblende to wurtzite [4]. This is promising since the growth of Sn-seeded GaAs in other research has yet to show the wurtzite phase [19] [5].

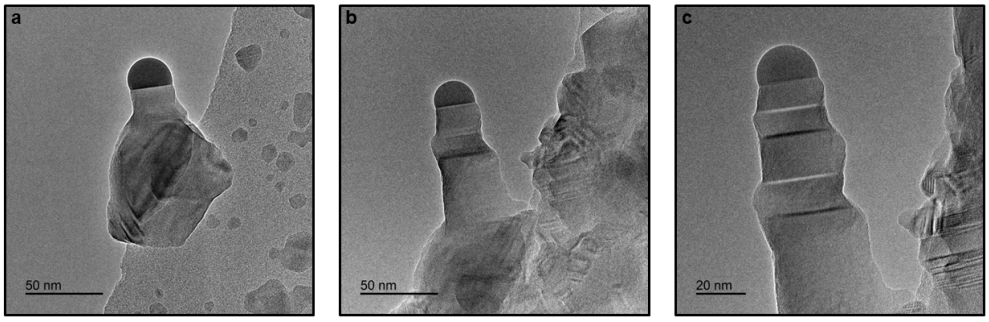

Figure 10: (a) Showing normal zincblende growth at the higher V/III ratio. (b) Showing when the V/III ratio was lowered. (c) Zoomed in image when the twin superlattice had grown out.

5.1.1. Overgrowth

When using TMGa and AsH_3 some issues with overgrowth on the substrate were encountered. This overgrowth can be divided into two categories: precursor related and substrate/seed particle related.

The former implies that there was substantial radial overgrowth superseding the axial growth, which suggest not optimal growth conditions, however this was an issue at all of the experiments conducted. There were several occurrences where the Ga and As concentration in the seed particle was at approximately the range of the detection

limit for the EDX [22], perhaps indicating that the supersaturation was not a substantial amount higher at the seed particle than at other locations. This would mean that there is not a kinetic driving force that promotes axial growth of nanowires as the preferred growth. An example of the overgrowth is shown in Figure 11, where it also appears that perhaps it was electron beam induced since the area around the image was not as affected.

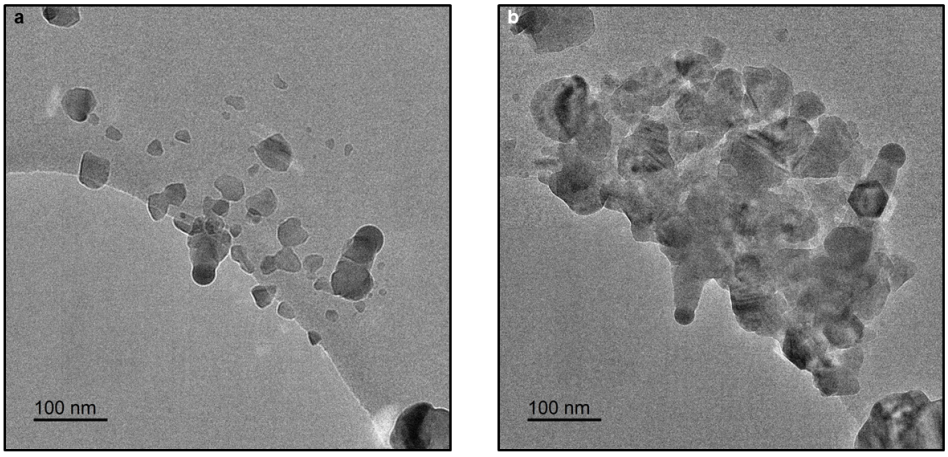

Figure 11: (a) Before overgrowth (b) After overgrowth (The images were taken 25 minutes apart.)

The substrate/seed particle related overgrowth can be due to agglomerates of the Sn particles that grow in multiple directions and form islands, as well as contamination metal particles which could also become a site for nucleation. On some regions of the chips that were used there appeared to be an uneven surface, which can be preferential sites to nucleate.

An additional issue that was often encountered was that the Sn particles seemed to 'disappear', an example of this is shown in Figure 12, where a tapered nanowire has no apparent particle left. Although Sn is a group IV element and is an amphoteric, there has been reports of Sn being a donor, therefore n-doping GaAs [6], it is not straightforward to examine if the Sn has doped the GaAs. The Sn could also have diffused along the substrate, but it is difficult to say with certainty what occurred. If the entire Sn particle would be incorporated it should show up in EDX so it is perhaps more probable for it diffusing away from the wire.

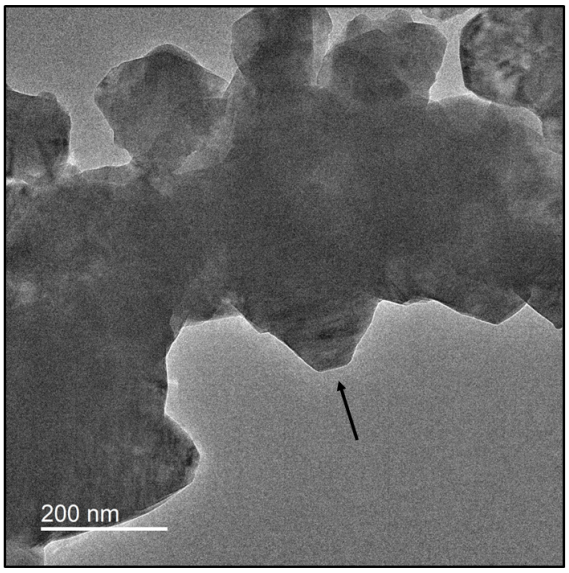

Figure 12: Another example of overgrowth and Sn particle that disappeared, the arrow indicates where the particle was located before.

5.1.2. Attempting a switch to GaSb

In one of the experiments where several Sn-seeded GaAs nanowires had nucleated and grown, there was an attempt at creating a heterostructure and switching to GaSb.

But firstly a promising nanowire was found that was growing axially into vacuum, at a temperature of 345 °C and partial pressures for TMGa: $3.03 \cdot 10^{-4}$ Pa and AsH_3: $1.43 \cdot 10^{-1}$ Pa shown in different magnifications in panel (a) and (b) in Figure 13. It was confirmed by EDX to be a Sn-seeded GaAs nanowire.

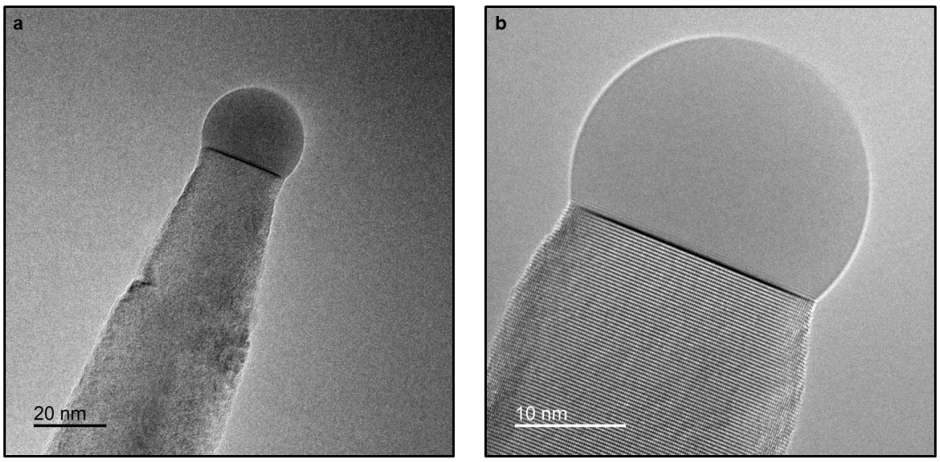

Figure 13: (a) Showing a GaAs nanowire at 500k magification. (b) Showing the same nanowire at a 1.5Mx magnification.

An overview image of the hole and the same nanowire studied is shown in panel (a) in Figure 14. The switching process was done as described in Section 4.3, lowering the temperature, stopping gas flows and purging before supplying gasses again. After approximately 90 minutes the partial pressures of TMGa and TMSb were $4.63 \cdot 10^{-3}$ Pa and $1.06 \cdot 10^{-1}$ Pa respectively and the temperature was 405 °C. The same hole is shown in panel (b) of Figure 14. Note that the nanowire had kinked, indicating suboptimal growth and transition conditions. Moreover the other nanowire that still had its seed particle in the hole after the switch was determined to be Ga-seeded by EDX.

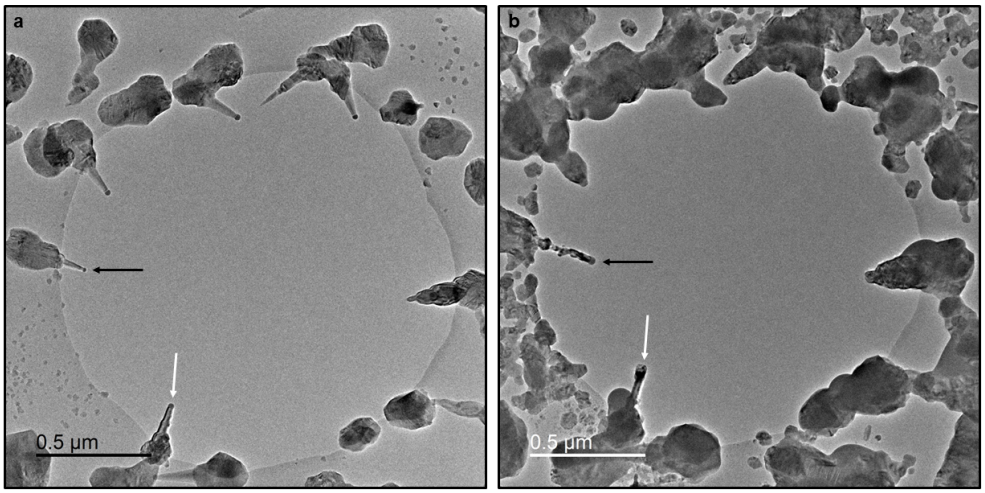

Figure 14: (a) Showing an overview image of a hole. Note the nanowire that is pointed out with a white arrow is Sn seeded. And the black arrow indicated Ga-seeded. (b) Showing an overview image of the same hole after changing to TMSb instead of ASH_3. Note that the same nanowires are pointed out with arrows

STEM-EDX mapping was used to confirm the incorporation of Sb, see Figure 15. It is clearly shown that Sb has been integrated, however, it kinked in such a way that made it difficult to know if the transition to pure GaSb was achieved.

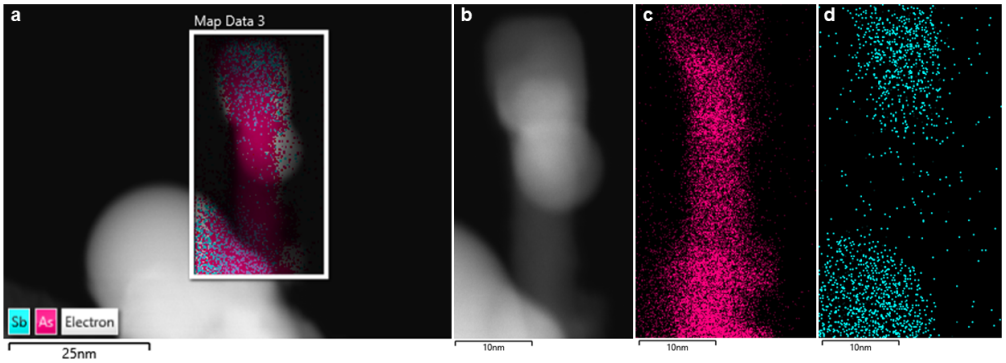

Figure 15: (a) Showing both As and Sb concentration for the nanowire pointed out with a white arrow in both panels in Figure 14. (b) Showing the nanowire studied. (c) Showing only As concentration. (d) Showing only the Sb concentration.

5.2. Growth of GaSb and switching to GaAs

The first step was to nucleate from Sn particles. A multitude of growth conditions were surveyed, which did not result in nucleation. However, after some time the optimal conditions where a majority of particles had nucleated were found. An example of the nucleated particles is shown in Figure 16. Although some nanowires had nucleated before, the majority were nucleated at 360 °C and partial pressures of TMGa $3.28{\cdot}10^{-3}$ Pa TMSb and $1.85{\cdot}10^{-2}$ Pa.

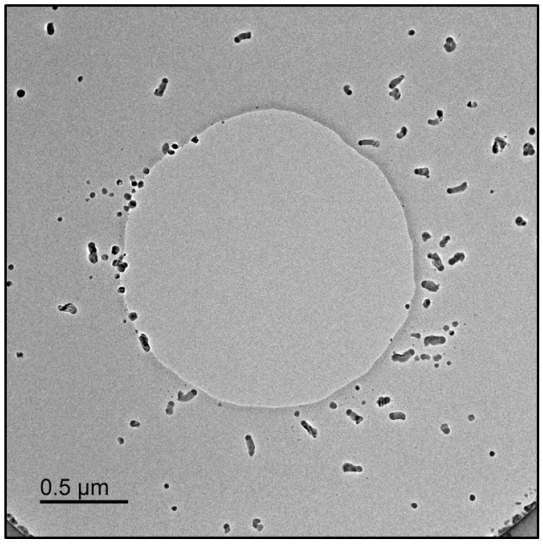

Figure 16: Image of a hole showcasing nucleated particles.

The same temperature and partial pressures were kept for the nanowire growth as the nanowires were growing axially and without kinking. Two nanowires that were growing out towards vacuum were observed and can be seen in panel (a) in Figure 17.

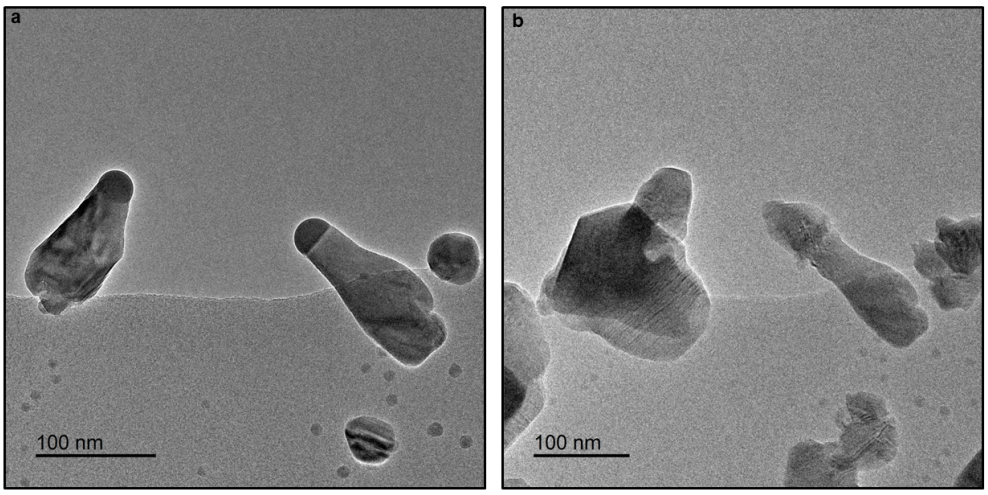

Figure 17: (a) Two GaSb nanowires (b) The same two nanowires. Note the loss of Sn particles and the overgrowth on the nanowire to the left in each image.

The system was prepared for a switch by lowering the temperature, stopping the gasses and purging the lines to then supply TMGa and AsH_3 with partial pressure of $1.71 \cdot 10^{-3}$ Pa and $4.71 \cdot 10^{-1}$ Pa respectively and a temperature of 360 °C. After the switch, there were nanowires that had lost their particle, an example is shown in Figure 17 in panel (b). However, there were examples of wires with the particle still intact and one of them was observed in Figure 18 in panel (a). What is interesting to note is the structure of the nanowire, at the bottom, almost round part, there appeared to be a crystal part underneath a top layer in the shape of a polygon. Since this could indicate that there were two different layers, the composition of different parts of the structure was determined by EDX and spectra were collected at four parts of the structure. The results are shown by circles in Figure 18 in panel (a), there is also a graph showing the As and Sb concentration of the different corresponding areas in panel (b). Note especially the values of the third area, there is a significant amount of Sb, where it was previously mentioned that there appeared to be some structure below a top layer. This suggests that there perhaps was GaSb underneath and that the GaAs overgrew on top of the GaSb. As mentioned in Section 5.1.1 there were many cases where the GaAs overgrew which makes this assumption plausible. The three other areas are pure GaAs and this indicates that the switch was partly successful, although it was not possible to follow the switch due to the shape of the nanowire.

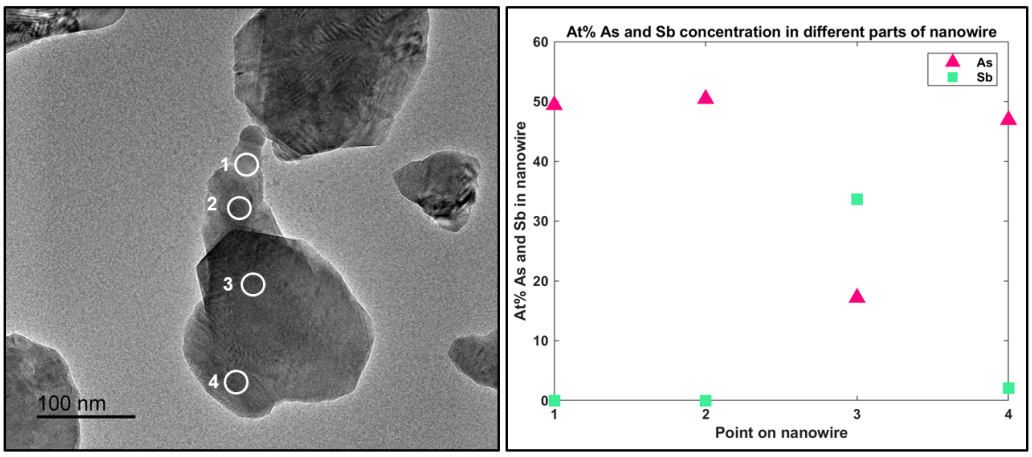

Figure 18: (a) Nanowire on the SiNx film after the GaAs switch. The circles mark areas from which EDX spectra were recorded. (b) Graph showing the As and Sb content throughout the wire.

5.3. Formation of GaSb-GaAs-GaAsSb nanowire heterostructures

After attempting to grow a heterostructure GaSb-GaAs in the aforementioned experiment, another attempt was made with a different approach and two switches were performed.

5.3.1. Starting with GaSb

Using similar conditions as in the end of Section 5.2, since it produced axial, non-kinked nanowires, an observed nanowire nucleated. This meant a TMGa partial pressure of $2.6{\cdot}10^{-3}$ Pa and for TMSb $2.93{\cdot}10^{-2}$ Pa. A nanowire had nucleated as shown in panel (a) of Figure 19. Nonetheless, other particles had not been nucleated in this experiment with the conditions used and it was speculated that the supersaturation was not achieved. Therefore, the conditions were altered and the TMGa flow was increased to a partial pressure of $4.27{\cdot}10^{-3}$ Pa, and TMSb was at $2.41{\cdot}10^{-2}$ Pa, to increase the Ga content in the particle [23]. This resulted in further nucleation of other particles as can be shown in panel (b) in Figure 19. It cannot be excluded that the growth time affects the yield of nucleation as has been shown by M. Tornberg et al. [5]. Their research showed that if a layer of GaSb covers the surface it results in higher nucleation yield. Subsequently the nanowire growth was considered to be slow, and the TMGa flow was lowered again which resulted in the first conditions mentioned in this section. EDX analysis confirmed that the particle composition during growth was: Ga 27.34 at.%, Sn 68.55 at.% and Sb

4.11 at.%.

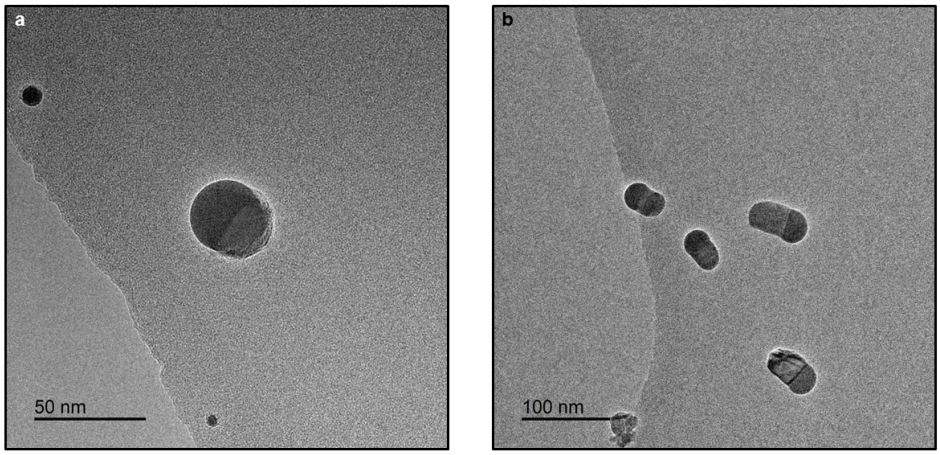

Figure 19: (a) First observed nucleation of Sn seeded GaSb. (b) When more particles had nucleated at altered conditions.

5.3.2. Switch to GaAs

A nanowire (NW # 1) growing into vacuum was chosen to be observed, see panel (a) in Figure 20, since this allowed for tilting the sample and observing atomic resolution. As can be seen on the sides of the nanowire there is a contamination layer which can be speculated to be a carbon layer due to the use of two trimethyl-III sources and that carbon can also be released in the disassociation process as described in Section 3.1.

After the nanowire had grown out as seen in panel (a) in Figure 20, a switch to GaAs was attempted as described in Section 4.3, however it was decided to withhold the purging to cause a more gradual transition. As mentioned in Section 5.2 the transition in that experiment seemed to have occurred between GaSb and GaAs but it was not distinct and the overgrowth was an issue. It was believed that if As was incorporated while Sb was still in the line, the transition could result in a still axial nanowire. There is also an inherent difficulty in matching two different materials together due to lattice mismatch which can lead to strain and defects [3].

When the other materials were introduced to the system the partial pressures of TMGa was $1.4{\cdot}10^{-3}$ Pa and for AsH_3 $1.83{\cdot}10^{-1}$ Pa, the temperature was set to 360 °C. During this switch the nanowire kinked which can be seen in panel (b) of Figure 20. By performing Fast Fourier Transform (FFT) analysis, it was confirmed that it was growing zincblende from viewing direction [110] in a <111> direction. The angle was measured to be approximately 70.5 °which agrees with the angle between two members of the

<111> directions of the same polarity. It is not possible to determine whether it was <111A> or <111B> directly as the nanowires grew on an amorphous substrate and not on a designated polarized substrate. There are also accounts of both kinds of polarities when growing Sn-seeded GaSb nanowires from former research by R. Zamani et.al. [24].

The kinking is unwanted since the aim is to use these types of structures for electronic devices where defects interrupt and worsen the electrical properties [3]. This means that there needs to be further investigation into how to optimise the switch and growth. When the nanowire had grown approximately 50 nm from the kink, a twin superlattice structure appeared as had also been observed before as mentioned in Section 5.1. Right before the first twin appeared, the composition was confirmed to be pure GaAs. EDX analysis of the particle showed that the composition was Ga 0.92 at.%, Sn 97.82 at.% and As 1.26 at.%. There seemed to be a drastic change in the Ga content of the seed particles when growing GaSb and GaAs. One proposal that could be implemented is to deplete the particle of Ga before the switch since there have been several observations of Sn-seeded GaAs growth that grows axially and without visible defects with very little Ga in the particle. The kink that occurred in Section 5.1.2 for the attempted GaAs-GaSb perhaps also happened due to this difference. It could be that when the particle quickly accumulated Ga (going from GaAs to GaSb) it fell off the nanowire.

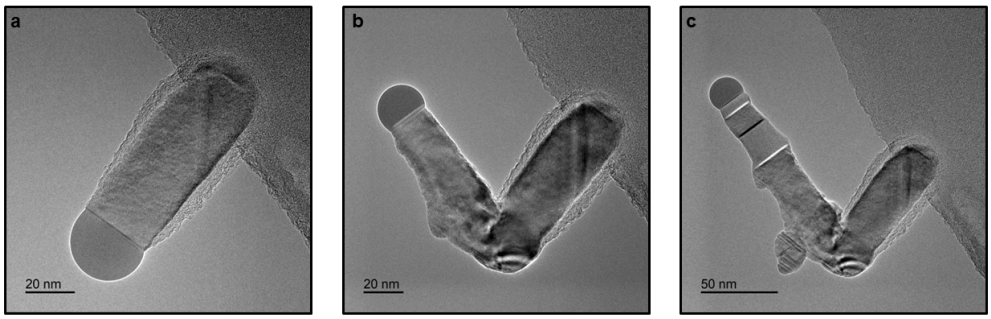

Figure 20: (a) Pure GaSb nanowire. (b) Kinked nanowire after switching to AsH_3. (c) When reaching pure GaAs twinning was present in the nanowire.

Returning to the twin phenomenon observed in the GaAs part, it had been noticed before in Section 5.1. For the experiment in this section, the V/III ratio was 120, even lower than it was in the previous experiment. However, that experiment was also done at a different temperature (385 °C), which means that they cannot be directly correlated.

The transition from GaSb to GaAs will be discussed in further detail below.

5.3.3. Switch to GaAsSb

When the GaAs had grown out approximately 100 nm, a switch to TMSb instead of AsH_3 was prepared as described in Section 4.3, however the lines were not purged but just

emptied. The intention of this was, as described from the first switch of the structure, to cause a more gradual transition. Moreover, in the transition attempted in Section 5.1.2 it led to a kinked nanowire after purging the lines, which was also a contributing reason for not purging them in this case. The partial pressure of TMGa was $2.72 \cdot 10^{-3}$ Pa and AsH_3 $3.13 \cdot 10^{-2}$ Pa and the temperature was again 360 °C. The morphology of the nanowire can be seen in Figure 21.

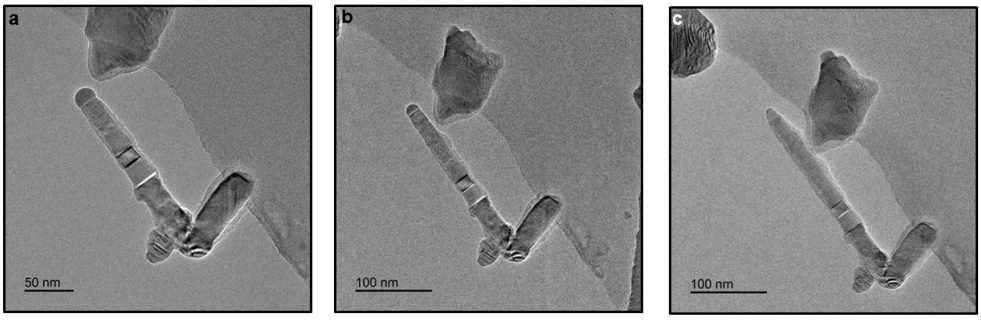

Figure 21: (a) 17 min after starting the TMSb supply. (b) 33 min after. (c) 120 minutes after.

The composition of the nanowire (NW # 1) was followed by collecting several EDX spectra minutes apart, in addition another nanowire (NW # 2, shown in panel (c) in Figure 23) was also studied in the same way. The results are illustrated in Figure 22 and shows that there was a ternary transition and that the As lingered in the system for some time. However, the last measurement showed that there was close to pure GaSb, with 3 at.% As for NW # 1. For NW # 2 there was approximately the same amount of As left in the nanowire at the end of the experiment, but the first value of As was lower than the second, while the Sb was higher for the first point than the second which could be considered odd, this can be seen in Figure 22. This could be attributed to the fact that there is an inherent insecurity when choosing an area to perform EDX on since it is done manually and tried to be done right underneath the seed particle. Nonetheless, the two nanowires generally showed a decrease of As content as the nanowire grew.

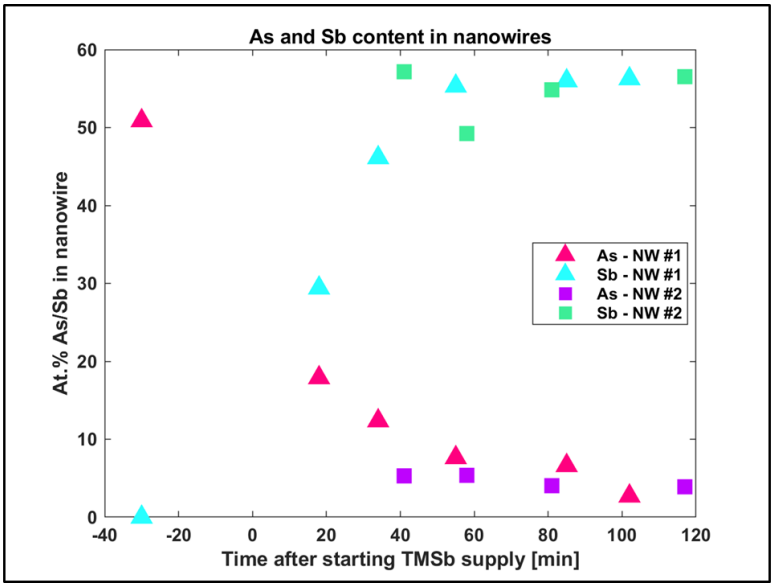

Figure 22: This graph shows how the As and Sb content varied for two nanowires right underneath the particle as time progressed after starting the supply of TMSb.

Referring back to Figure 21, there has been tapering and great reduction of seed particle volume in panel (c). There are multiple possibilites as to what occurred. Sn could have diffused along the nanowire and left the nanowire. Another possible reason is that Sn perhaps doped the nanowire as mentioned before with GaAs. In bulk GaSb, Sn has been shown to be an acceptor [5], and there are studies showing that Sn also acts as an acceptor in GaSb when crystals were grown by Molecular Beam Epitaxy [25]. This is an indicator that it would also p-dope GaSb nanowires, but it is difficult to know for certain. If it were to act as an acceptor it would not be an unfavorable property, since GaSb is mainly hole mobility based. However, the droplet shrinking is suboptimal since it changes the morphology of the nanowire and can change the growth behavior. There has been research showing that Sn has doped GaAs nanowires as mentioned previously [19], so it should not be impossible for it to dope GaSb as well.

Moreover, when studying different holes the shape of the nanowires indicate that at least the Sb was started to be incorporated due to the apparent radial increase, pointed out by arrows in Figure 23. The same result has been found before, e.g. in M. Borgs et.al. work about antimonide nanowires [2]. The nanowire (NW # 1) that was extensively studied did not show this behavior of radial increase, however, that could be due to the fact that there was an apparent contamination layer capping it. NW # 2 showed this behavior and is shown in panel (c) of Figure 23. This phenomenon is pointed out as it can be speculated to give an indication to the yield of how the transition worked even if there was no EDX performed at each of the wires. It is also worth mentioning that most of these nanowires, pointed out with arrows, have island-like structures at the bottom, although they grew out axially - perhaps indicating that the first switch (GaSb-GaAs) did not result in axial growth. While the nanowire that was extensively studied in it

kinked. This all means that the transition (GaSb-GaAs) needs to be further investigated and optimized.

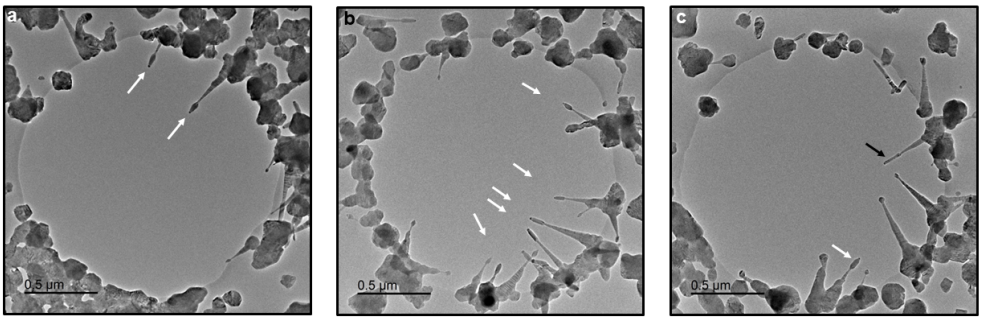

Figure 23: (a) Overview image over a hole after both switches. (b) Overview image over another hole after both switches. (c) Overview over the hole where the two nanowires studied above were located. The black arrow points at NW # 2.

5.3.4. STEM mapping

For the nanowire that was shown in Figures 20 and 21, the entire composition of the nanowire was studied by acquiring a STEM map over several hours, resulting in Figure 25. This was thought to be an approach to e.g. see Sn in the nanowire, however, the amount of Sn detected was at the limit of what the EDX can resolve which makes it difficult to confirm that the Sn indeed doped the structure. There was not a really clear characteristic Sn peaks in the STEM map, as can be seen in Figure 24, which corresponds to the pink area marked in Figure 25. The Sb and Sn signal overlaps as well which can make it difficult to know for sure although the acquisition time was several hours which could be considered as enough.

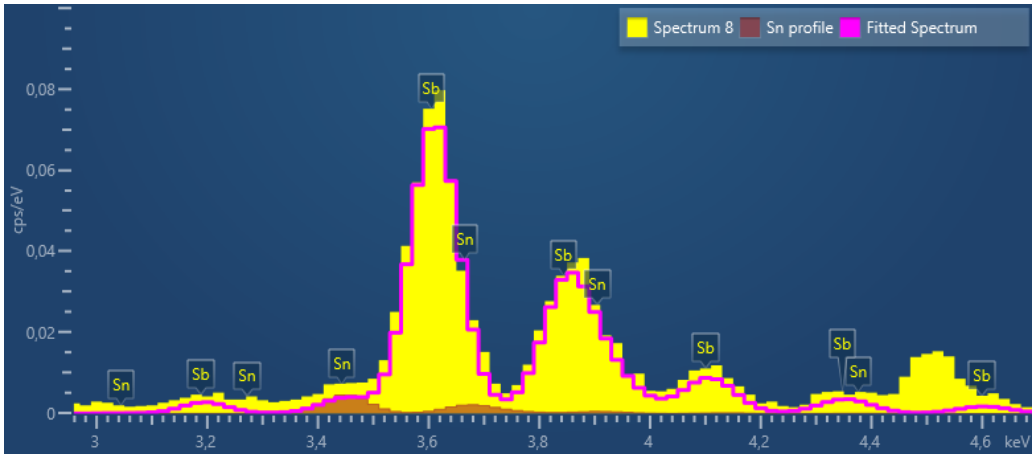

Figure 24: Spectrum of an area corresponding to the pink rectangle in Figure 25.

Moreover, the most important takeaway from STEM mapping was to study the material transitions that had been performed. The gallium content was consistent throughout the structure, so it was considered to be of advantage to show the Sb and As to follow the switch.

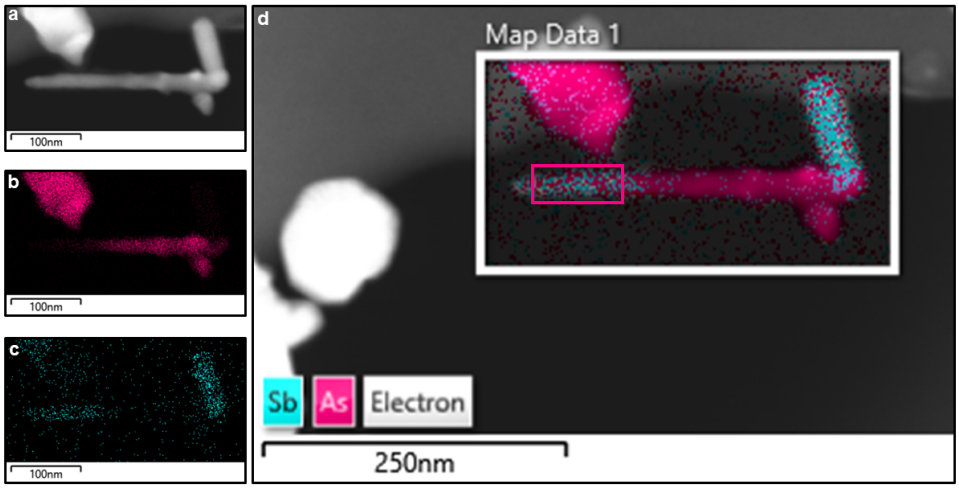

Figure 25: (a) STEM image of nanowire (b) Showing the As concentration of the nanowire. (c) Showing the Sb concentration of the nanowire. (d) Showing both As and Sb concentration together.

In the first transition the kink occurred and it was here that the lines were not purged or emptied before AsH_3 was supplied. Sb can be seen to have a prominent concentration right up until the kink and here is a small area of the nanowire where the As and Sb overlap and the bump right after the kink appears to be GaAs. Even though the Sb seemed from the STEM map to have left the nanowire shortly after the kink, it grew out about 50 nm before twinning was observed as mentioned previously. It could be considered strange that the twinning did not start earlier, however, it must be noted that the detection limit for EDX in the system is around 1 at.% which means that there might have still been Sb within the wire. Moreover, Sb has been shown to linger in reactors due to its low vapor pressure, which makes it difficult to know when or if it left [2]. It has been speculated that there seems to be a higher supersaturation for GaAs than GaAsSb, i.e. a larger thermodynamic driving force for growing [26], which could have facilitated the transition. In any case for future reference, it would be necessary to pump down the system longer in order to give Sb more time to leave.

For the second transition, as mentioned previously, the lines were emptied of ASH_3 but not purged. In the STEM map it is clear that the As lingered for quite some time in the nanowire which also coincides with the point EDX spectra taken during the growth from Figure 22. It is clear that the As did not fully leave and this was considered

somewhat unanticipated since there have been multiple reports of successful GaAs-GaSb heterostructures [5][4]. However, in the mass spectrometer, RGA, used there was a constant of AsH_3 in the system, a magnitude lower than for Sb, in the beginning when TMSb was supplied. It is worth noting that the RGA is located at the exhaust of the gas line and therefore the gas might have been diluted when reaching that point. Nonetheless, it could be speculated that the As somehow increases the supersaturation in comparison to Sb and therefore in this system, meaning that GaAs has lower chemical potential and therefore indicating that GaAsSb is preferred over GaSb. As mentioned before since GaAs can be preferred over GaAsSb due to higher supersaturation [26], this could perhaps indicate that GaAsSb is more preferred than GaSb, however, this is a complex process and would need further investigation to be confirmed.

5.4. Overview of results for heterostructure transitions

After describing the different attempts at creating heterostructures with GaAs and GaSb, it can be beneficial to have a look at an overview over what was done, see Table 2.

GaAs-GaSb #1 is described in Section 5.1.2 where the transition was kinked but Sb was confirmed to be incorporated into the nanowire. Before the switch the lines were purged. The second attempt of this transition is described in Section 5.3.3 and it resulted in a GaAs-GaAsSb heterostructure. Different parameters were used and it was decided to not purge but only empty the line of residual gas which caused a more gradual transition and no kink, however pure GaSb was not reached which was the goal, perhaps an attempt at emptying the ASH_3 would lead to a better result.

GaSb-GaAs #1 is described in Section 5.2 and the conditions used resulted in loss of Sn particles, overgrowth when switching to GaAs and one example of a possibly successful transition from GaSb to GaAs. Before the switch the lines were purged. The second attempt at a transition from GaSb-GaAs is described in Section 5.3.2, and it was decided not to purge or empty the lines - leaving all of the residual TMSb in the lines when AsH_3 entered, since this was thought to perhaps hinder the overgrowth of GaAs and leave a still axial nanowire. This lead to a gradual transition and a kinked nanowire, however pure GaAs was reached and the composition could be followed afterwards with STEM mapping. To avoid kinking in the future, perhaps the Sn particle needs to be depleted from Ga since particle EDX for GaSb showed high Ga content and low Ga content for GaAs.

Table 2: Overview table of the heterostructure transitions.

Material transitions → **Parameters/Comments ↓**	**GaAs-GaSb #1**	**GaSb-GaAs #1**	**GaAs-GaAsSb**	**GaSb-GaAs #2**
Purging or not	Purged the line	Purged the line	Did not purge but emptied the line	Did not purge or empty the line
Temperature	Before switch: 345°C After switch: 405°C	360°C	360°C	360°C
Partial pressures before switch [Pa]	TMGa: $3.03 \cdot 10^{-4}$ AsH_3: $1.43 \cdot 10^{-1}$	TMGa: $3.28 \cdot 10^{-3}$ TMSb: $1.85 \cdot 10^{-2}$	TMGa: $1.4 \cdot 10^{-3}$ AsH_3: $1.83 \cdot 10^{-1}$	TMGa: $2.6 \cdot 10^{-3}$ TMSb: $2.93 \cdot 10^{-2}$
Partial pressures after switch [Pa]	TMGa: $4.63 \cdot 10^{-3}$ TMSb: $1.06 \cdot 10^{-1}$	TMGa: $1.71 \cdot 10^{-3}$ AsH_3: $4.71 \cdot 10^{-1}$	TMGa: $2.73 \cdot 10^{-3}$ TMSb: $3.13 \cdot 10^{-2}$	TMGa: $1.4 \cdot 10^{-3}$ AsH_3: $1.83 \cdot 10^{-1}$
Comments	Kinked, Ga-seeded nanowires, not many intact nanowires after switch	Loss of Sn. Overgrowth when switching to GaAs - possible 'partly successful transition'	As did not leave the wire, no kink	Kinked, reached pure GaAs

6. Conclusions and outlook

Sn-seeded GaAs and GaSb nanowires have been grown and their growth conditions have been studied and experimented with, to later switch materials and create heterostructures.

Twinning in GaAs nanowires was found at lower V/III ratios where the trend seemed to coincide with ex-situ work, which also shows promising polytypism behavior in Sn-seeded GaAs. A great issue with GaAs was overgrowth that hindered the optimization of the nanowire growth, and is speculated to have a correlation with the apparent lack of As and Ga in the particle nanowire indicating that it is not entirely thermodynamically favorable to grow axial nanowires. Nonetheless, a switch was made from GaAs to GaSb that resulted in a kinked nanowire indicating that the growth conditions were non-ideal.

Starting with GaSb switching to GaAs it appeared to have lead to a partly successful switch, pure GaAs was achieved after examining it with EDX, however, the overgrowth of GaAs was a considerable problem and the yield of nanowires with their Sn particle left was low.

With the studies performed of GaAs-GaSb and GaSb-GaAs, there was a background and several insights that could aid in choosing the optimal growth conditions, and a GaSb-GaAs-GaAsSb heterostructure was created. For the first switch of the GaSb-GaAs-GaAsSb nanowire - GaAs-GaSb, the nanowire kinked, meaning that these growth conditions need to be optimized further. Approximately 50 nm after the nanowire had

kinked a twin superlattice structure appeared and it was confirmed to be pure GaAs. From the STEM map it appeared as though Sb left the system relatively quickly, however, there is a detection limit for the EDX system which might mean there was still some Sb in the nanowire. Moreover, as mentioned it has also been reported that Sb affects the crystal growth even if not incorporated into the crystal. These could be reasons as to why it took some time for the twin superlattice to form.

For the second switch of the same nanowire, GaAs-GaAsSb, a pure GaSb was the aim but As stayed in the nanowire. Due to a background of As this was not unexpected. Since other research has shown that As appears to give a higher supersaturation than Sb, making it more preferred, could also be an explanation as to why As stayed within the nanowire.

There are many possibilities for future research concerning GaAs and GaSb heterostructures. First and foremost there is a need to find a way to avoid the kinking from GaSb to GaAs, for example by trying to deplete the Ga from the particle before switching as mentioned before. Furthermore, there is a need to achieve pure GaSb after switching from GaAs, to recreate and optimize in-situ results to compare them with ex-situ work which can help with translating the methods into each other. More studies can also be made to study the particle composition difference between Sn-seeded GaAs and GaSb to further explore how it can help to optimize the growth parameters. It would also be interesting to try to form the heterostructure GaAs-GaSb-GaAs, which would in theory create a quantum dot due to the band gap difference between GaAs and GaSb. The promising results of combining Sn-seeded GaAs and GaSb nanowires in-situ and understanding the processes together with their possible applications, shows a need for future in-situ investigation. The work done in this thesis is a great foundation for such endeavours.

References

[1] Enrique Barrigón, Magnus Heurlin, Zhaoxia Bi, Bo Monemar, and Lars Samuelson. Synthesis and applications of iii–v nanowires. *Chemical Reviews*, 119, 2019.

[2] Mattias Borg and Lars-Erik Wernersson. Synthesis and properties of antimonide nanowires. *Nanotechnology*, 24(20):202001, 2013.

[3] Maria de la Mata, César Magén, Philippe Caroff, and Jordi Arbiol. Atomic scale strain relaxation in axial semiconductor III-V nanowire heterostructures. *Nano Letters*, 14, 2014.

[4] Mattias Borg, Kimberly Dick, Jakob Wagner, Philippe Caroff, Knut Deppert, Lars Samuelson, and Lars-Erik Wernersson. GaAs/GaSb nanowire heterostructures grown by MOVPE. *Journal of Crystal Growth*, 310:4115–4121, 2008.

[5] Marcus Tornberg, Erik K Mårtensson, Reza R Zamani, Sebastian Lehmann, Kimberly A Dick, and Sepideh Gorji Ghalamestani. Demonstration of sn-seeded gasb homo- and gaas–gasb heterostructural nanowires. *Nanotechnology*, 27(17):175602, 2016.

[6] Rong Sun, Daniel Jacobsson, I-Ju Chen, Malin Nilsson, Claes Thelander, Sebastian Lehmann, and Kimberly A. Dick. Sn-seeded GaAs nanowires as self-assembled radial p-n junctions. *Nano Letters*, 15, 2015.

[7] Marcus Tornberg, Carina B. Maliakkal, Daniel Jacobsson, Reine Wallenberg, and Kimberly A. Dick. Enabling in situ studies of metal-organic chemical vapor deposition in a transmission electron microscope. *Microscopy and Microanalysis*, 28(5):1484–1492, 2022.

[8] Udo W. Pohl. *Epitaxy of Semiconductors—Introduction to Physical Principles*. Wiley-VCH, 2013.

[9] R. S. Wagner and W. C. Ellis. Vapor-Liquid-Solid Mechanism Of Single Crystal Growth. *Applied Physics Letters*, 4(5):89–90, 1964.

[10] Kimberly Dick. A review of nanowire growth promoted by alloys and non-alloying elements with emphasis on Au-assisted III-V nanowires. *Progress in Crystal Growth and Characterization of Materials*, 54:138–173, 2008.

[11] Vladimir G. Dubrovskii. *Nucleation Theory and Growth of Nanostructures*. NanoScience and Technology. Springer Berlin, Heidelberg, 2014.

[12] Sepideh Gorji Ghalamestani, Sebastian Lehmann, and Kimberly A. Dick. Can antimonide-based nanowires form wurtzite crystal structure? *Nanoscale*, 8:2778–2786, 2016.

[13] David B. Williams and C. Barry Carter. *Transmission Electron Microscopy: A Textbook for Materials Science*. Springer, New York, NY, 2 edition, 2009.

[14] R.F. Egerton. *Physical Principles of Electron Microscopy: An Introduction to TEM, SEM, and AEM*. Springer, Cham, 2 edition, 2016.

[15] Stephen J. Pennycook and Peter D. Nellist, editors. *Scanning Transmission Electron Microscopy: Imaging and Analysis*. Springer, New York, NY, 1 edition, 2011.

[16] Crispin Hetherington, Daniel Jacobsson, Kimberly A Dick, and L Reine Wallenberg. In situ metal-organic chemical vapour deposition growth of iii–v semiconductor nanowires in the lund environmental transmission electron microscope. *Semiconductor Science and Technology*, 35(3):034004, 2020.

[17] James Y Howe, Michael S Thompson, Selim Dogel, Kazuhiro Ueda, Toshio Matsumoto, Hiroaki Kikuchi, Michael Reynolds, Hossein Hossainkhannazer, and Thomas J Zega. In situ thermal shock of lunar and planetary materials using a newly developed MEMS heating holder in a STEM/SEM. *Microscopy and Microanalysis*, 23:66–67, 2017.

[18] R. T. Hallberg, L. Ludvigsson, C. Preger, B. O. Meuller, K. A. Dick, and M. E. Messing. Hydrogen-assisted spark discharge generated metal nanoparticles to prevent oxide formation. *Aerosol Science and Technology*, 52(3):347–358, 2018.

[19] Rong Sun, Daniel Jacobsson, I-Ju Chen, Malin Nilsson, Claes Thelander, Sebastian Lehmann, and Kimberly. A. Dick. Sn-seeded GaAs nanowires as self-assembled radial p–n junctions. *Nano Letters*, 15(6):3757–3762, 2015. PMID: 25989532.

[20] Erik K. Mårtensson, Sebastian Lehmann, Kimberly A. Dick, and Jonas Johansson. Simulation of gaas nanowire growth and crystal structure. *Nano Letters*, 19(2):1197–1203, 2019.

[21] F. Glas, J. C. Harmand, and G. Patriarche. Why does wurtzite form in nanowires of III-V zinc blende semiconductors? *Phys. Rev. Lett.*, 99:146101, 2007.

[22] C.B. Maliakkal, D. Jacobsson, M. Tornberg, et al. In situ analysis of catalyst composition during gold catalyzed gaas nanowire growth. *Nature Communications*, 10(1):4577, 2019.

[23] Carina B. Maliakkal, Erik K. Mårtensson, Marcus Ulf Tornberg, Daniel Jacobsson, Axel R. Persson, Jonas Johansson, Lars Reine Wallenberg, and Kimberly A. Dick. Independent control of nucleation and layer growth in nanowires. *ACS Nano*, 14(4):3868–3875, 2020. PMID: 32049491.

[24] Reza R. Zamani, Sepideh Gorji Ghalamestani, Jie Niu, Niklas Sköld, and Kimberly A. Dick. Polarity and growth directions in Sn-seeded GaSb nanowires. *Nanoscale*, 9:3159–3168, 2017.

[25] K. F. Longenbach, S. Xin, and W. I. Wang. p-type doping of GaSb by Ge and Sn grown by molecular beam epitaxy. *Journal of Applied Physics*, 69(5):3393–3395, 1991.

[26] DL Dheeraj, Gilles Patriarche, Hailiang Zhou, Thang B Hoang, Alex F Moses, Siri Grønsberg, Antonius T van Helvoort, Bjørn-Ove Fimland, and Helge Weman. Growth and characterization of wurtzite GaAs nanowires with defect-free zinc blende GaAsSb inserts. *Nano Letters*, 8(12):4459–4463, 2008.